Atmos. Chem. Phys. Discuss., 15, 4083–4115, 2015
www.atmos-chem-phys-discuss.net/15/4083/2015/
doi:10.5194/acpd-15-4083-2015


Atmospheric Chemistry and Physics Discussions



# Regional differences in Chinese $SO_2$ emission control efficiency and policy implications

**Q. Q. Zhang[1,2], Y. Wang[1,3,4], Q. Ma[1,2], Y. Xie[1], and K. He[2]**

[1]Ministry of Education Key Laboratory for Earth System Modeling, Center for Earth System Science, Institute for Global Change Studies, Tsinghua University, Beijing, China
[2]School of Environment, Tsinghua University, Beijing, 100084, China
[3]Department of Marine Sciences, Texas A&M University at Galveston, Galveston, TX, 77553, USA
[4]Department of Atmospheric Sciences, Texas A&M University, College Station, TX, 77843, USA

Received: 13 January 2015 – Accepted: 27 January 2015 – Published: 12 February 2015

Correspondence to: Y. Wang (yxw@tsinghua.edu.cn)

Published by Copernicus Publications on behalf of the European Geosciences Union.







## Abstract

$SO_2$ emission control has been one of the most important air pollution policies in China since 2000. In this study, we assess regional differences in $SO_2$ emission control efficiencies in China through the modeling analysis of four scenarios of $SO_2$ emissions, all of which aim at reducing the national total $SO_2$ emissions by 8 % or 2.3 Tg below the 2010 emissions level, the target set by the current 12th FYP (2011–2015), but differ in the spatial implementation. The GEOS-Chem chemical transport model is used to evaluate the efficiency of each scenario on the basis of three impact metrics: surface sulfate concentration, population-weighted sulfate concentration (PWC), and sulfur export flux from China to the Western Pacific. The efficiency of $SO_2$ control ($\beta$) is defined as the relative change of each impact metric to a 1 % reduction of $SO_2$ emissions from the 2010 baseline. The S1 scenario, which adopts a spatially uniform reduction of $SO_2$ emissions in China, gives a $\beta$ of 0.71, 0.83, and 0.67 for sulfate concentration, PWC, and export flux, respectively. By comparison, the S2 scenario, which implements all the $SO_2$ emissions reduction over North China (NC), is found most effective in reducing national-mean surface sulfate concentrations and sulfur export fluxes, with $\beta$ being 0.76 and 0.95 respectively. The S3 scenario of implementing all the $SO_2$ emission reduction over South China (SC) has the highest $\beta$ in reducing PWC ($\beta$ = 0.98) because SC has the highest correlation between population density and sulfate concentration. Reducing $SO_2$ emissions over Southwest China (SWC) is found to be least efficient on the national scale, albeit within-region benefit. The difference in $\beta$ by scenario is attributable to regional differences in $SO_2$ oxidation pathways and source–receptor relationships. Among the three regions examined here, NC shows the largest proportion of sulfate formation from gas phase oxidation, which is more sensitive to $SO_2$ emission change than aqueous oxidation. In addition, NC makes the largest contribution to interregional transport of sulfur within China and to the transport fluxes to Western Pacific. The policy implication is that China needs to carefully design a regionally specific implementation plan of realizing its $SO_2$ emissions reduction target in order to maximize






ACPD
15, 4083–4115, 2015



the resulting air quality benefits not only for China but for the downwind regions, with emphasis on reducing emissions from NC.

## 1 Introduction

$SO_2$ is the precursor of ambient sulfate, which is a major component of particulate matter with dynamic diameter less than 2.5 µm ($PM_{2.5}$) and makes up about 20–35 % of total $PM_{2.5}$ mass (Pathak et al., 2009). $SO_2$ emissions from China contribute about 25 % of global $SO_2$ emissions and 50 % of Asian emissions (Streets et al., 2003; Lu et al., 2011). Since 2000, the Chinese government has made great efforts in controlling $SO_2$ emissions in order to reduce atmospheric PM concentrations and acid deposition. A 10 % $SO_2$ emission reduction target was set in both the tenth five-year Plan (10th FYP, 2000–2005) and the 11th FYP (2006–2010). While $SO_2$ emissions increased about 28 % during the 10th FYP (Schreifels et al., 2012), by the end of the 11th FYP China has achieved the goal of 10 % $SO_2$ emission reduction in 2010 relative to the 2005 level (Lu et al., 2011). Itahashi et al. (2012a) reported that aerosol optical depths (AOD) retrieved from the Moderate Resolution Imaging Spectroradiometer (MODIS) over East Asia shows an increase from 2001 to 2005 and then a decrease until 2010, consistent with the reported trend of $SO_2$ emissions from China.

In 2012, $PM_{2.5}$ was introduced into China's ambient air quality standard by the Ministry of Environmental Protection (MEP). In response to severe haze pollution, the Action Plan on Prevention and Control of Air Pollution was delivered by the Central Government of China in September 2013. Aiming to improve air quality across China in the next five to ten years, the Action Plan calls for more efforts to reduce emissions from the heavily polluted regions in East China (22–42° N, 110–122° E). The Action Plan requires that by 2017, $PM_{2.5}$ concentrations should decrease by 25 % over the Beijing-Tianjin-Hebei region, 20 % over the Yangtze River Delta, and 15 % over the Pearl River Delta. While the Action Plan presents guidelines and advice for energy consumption and cleaner production, like other laws and regulations in China there is no specific





ACPD
15, 4083–4115, 2015



emission control target for primary PM or its gaseous precursors for the whole country or by specific regions.

The purpose of this study is to assess the regional differences in $SO_2$ emission control efficiency in China and discuss the implications for future emission control strategies. We chose three impact metrics to evaluate the efficiency of different scenarios of $SO_2$ emissions reduction in China. The first metric is surface sulfate concentration. The GEOS-Chem chemical transport model is used to quantify the response of sulfate concentrations to $SO_2$ emission change. Since public health is an important issue of concern for $PM_{2.5}$, the second metric is population-weighted sulfate concentration at the surface. $SO_2$ emissions from China also have significant impacts on air quality and public health of foreign regions due to long-range transport. Park et al. (2004) suggested that trans-Pacific transport of sulfate accounts for 30 % of sulfate background in the US. Itahashi et al. (2012b) reported that central eastern China is the dominant source region for sulfate aerosols over Oki Island during two air pollution events in July 2005. Previous studies have recognized the Western Pacific as the predominant transport pathway of air pollution exported from China (Heald et al., 2006; Fairlie et al., 2010; Li et al., 2010; He et al., 2012). Given the global impact of changing Chinese emissions, it is important to understand the response of pollution outflow to different emission control strategies in China. Therefore, the third metric is the outflow flux of sulfur from China to the Western Pacific.

Within the context of currently available emission control plans in China, we design four different spatial realizations of $SO_2$ reduction scenarios for China, all of which aim at reducing the national total $SO_2$ emissions by 8 % or 2.3 Tg below the 2010 emissions level, which is the target set by the current 12th FYP (2011–2015). In the first scenario $SO_2$ emissions are reduced uniformly by 8 % over China, while in the other three scenarios the emissions reduction is implemented over three different regions which have the largest contributions to the national $SO_2$ emissions and highest sulfate concentrations. Since sulfate aerosols exhibit regionally specific formation and trans-





ACPD
15, 4083–4115, 2015



port characteristics (Wang et al., 2013), the response of a given impact metric to the same amount of $SO_2$ emission reduction is expected to differ by region.

It is clear that the target of 8 % reduction of $SO_2$ emissions is far from sufficient to meet the goal of $PM_{2.5}$ concentrations set by the Action Plan (Wang et al., 2013). However, there is no other specific target of $SO_2$ emissions available in current Chinese policies to set as an alternative reference point. Since our study focuses on the regional difference in emission control efficiency, we choose an 8 % perturbation of total $SO_2$ emissions that is large enough to capture the regional difference.

The paper is organized as follows. Section 2 describes the model and the evaluation of model results by observations. In Sect. 3 we present the different reduction scenarios of $SO_2$ emissions in China and analyze the regionally different responses of the three impact metrics to those scenarios. Section 4 analyzes sulfate formation and sulfur transport by region to understand the mechanisms behind the regional differences of $SO_2$ emission control efficiency, followed by sensitivity tests of our results. The concluding remarks are presented in Sect. 5.

## 2 Model description and evaluation

### 2.1 Model description

We use the GEOS-Chem chemical transport model version 9-01-01 to simulate the coupled aerosol-oxidant chemistry on the global and regional scale. The model is driven by the assimilated meteorological data from the Goddard Earth Observation System (GEOS) with 6 h averaged winds, temperature, cloud and convective mass flux, and 3 h averaged surface quantities and mixing depths. Here we use the nested-grid capability of GEOS-Chem with a $0.5^\circ \times 0.667^\circ$ horizontal resolution over East Asia, which was originally described by Wang (2004) and Chen et al. (2009). The global simulation with a horizontal resolution of $4^\circ \times 5^\circ$ is used to provide boundary conditions for the nested-grid domain.





ACPD
15, 4083–4115, 2015



The sulfate-nitrate-ammonium (SNA) aerosol simulation coupled to the $HO_X$–$NO_X$–VOC-ozone gas chemistry was originally developed by Park et al. (2004). Emitted $SO_2$ in the model is oxidized to sulfate by hydroxyl radicals (OH) in the gas phase and by hydrogen peroxide ($H_2O_2$) and ozone ($O_3$) in the aqueous phase. The gas-particles equilibrium of aerosols is calculated using the ISOROPIA II (Fontoukis and Nenes, 2007) aerosol equilibrium model. The aerosols are removed through dry and wet deposition.

The Global Emission Inventory Activity (GEIA) inventory (Benkovitz et al., 1996) is used in the global simulation, which is overwritten by the NEI05 inventory over the US, the EMEP inventory over Europe, and the INTEX-B inventory over East Asia (Wang et al., 2013). For the nested-grid simulation, the Multi-resolution Emission Inventory for China (MEIC) for the year 2010 is adopted over China (He, 2012) and emissions over the rest of East Asia are taken from the INTEX-B emission inventory (Zhang et al., 2009). The MEIC inventory uses an improved technology-based methodology to estimate anthropogenic emissions from China, including emissions of $SO_2$, $NO_X$, $NH_3$, BC, OC, NMVOCs, CO, $CO_2$, and fine and coarse mode PM. The MEIC inventory has an open access dataset for the period from 1990 to 2010 (http://www.meicmodel.org), providing monthly emission data in the horizontal resolution of $0.25^\circ \times 0.25^\circ$, $0.5^\circ \times 0.5^\circ$ and $1^\circ \times 1^\circ$. The MEIC emission inventory is proved to be a good estimation of total emissions with some uncertainties in the spatial allocations for the fine grid resolutions within cities (Wang et al., 2014). According to the MEIC inventory, $SO_2$ emissions from China are 28.4 Tg in 2010 (Fig. 1).

### 2.2 Model evaluation

The GEOS-Chem simulation of sulfate and $PM_{2.5}$ over China has been evaluated by Wang et al. (2013, 2014) and Lou et al. (2014). Wang et al. (2013) presented that the GEOS-Chem model had a good performance in simulating sulfate distributions ($R^2 = 0.64 \sim 0.79$) and concentrations (mean bias of −10 %) in East Asia. Lou et al. (2014) reported a higher correlation between simulated and observed sulfate





ACPD
15, 4083–4115, 2015



($R^2$ = 0.86), but a larger model bias (−41 %) which may be partly due to the fact that they used a uniform factor of 0.6 to infer sulfate concentrations in $PM_{2.5}$ from that in observed $PM_{10}$ concentrations. Wang et al. (2014) further evaluated the model performance in reproducing the concentrations and the spatiotemporal patterns of $PM_{2.5}$ over China during a severely polluted month of January 2013. The model shows a good correlation of 0.6 with $PM_{2.5}$ distributions but underestimates the concentrations of $PM_{2.5}$ and sulfate over North China during the severe haze period, which is largely explained by underestimated emissions from this heavily polluted region. The sulfate underestimation is further attributed to the heterogeneous reaction of $SO_2$ on pre-existing aerosols that are deliquescent under the condition of higher relative humidity during the severe haze period (Wang et al., 2014). In this study we extend the previous model evaluation studies by using three additional datasets over China: (1) AOD retrieved from MODIS for January, July, and annual mean of 2010, (2) weekly-mean sulfate concentrations observed at the Miyun site (40°29′ N, 116°47′ N) from January to June 2010, (3) monthly wet deposition fluxes at 5 sites from January 2009 to December 2010, which are from the Acid Deposition Monitoring Network in East Asia (EANET, http://www.eanet.asia/).

The spatial distributions of AOD over China for 2010 annual mean, January and July from MODIS (top) and the model (bottom) are displayed in Fig. 2. The model shows a strong correlation ($R > 0.6$) with MODIS AOD, showing higher annual mean AOD in North and South China and the highest values shifting from central China in January to NC in July. The model has a positive bias of more than 10 % for the annual mean, January and July mean AOD levels over China as a whole. There is an obvious positive bias of the model over North China, with an overestimation of 26 and 20 %, respectively, for the annual mean and January. The model shows a higher correlation (0.73) and smaller bias (12 %) over North China in July. The model bias over South China and Southwest China is comparatively smaller and negative at −3 % for SC and −1 % for SWC. The positive bias of AOD in North China is due to the overestimates of





ACPD
15, 4083–4115, 2015



nitrate concentrations (Wang et al., 2013) and overestimation of dust emissions from the Taklimakan-Gobi area (Wang et al., 2012).

The simulated and observed weekly-mean sulfate concentrations from January to June 2010 at the Miyun site are compared in Fig. 3a. The model agrees well with the observed variability with a correlation of 0.75, and it shows a small positive bias of 4 % for sulfate concentration. Wang et al. (2013) reported an $R$ of 0.7 and overestimation of 15 % of the model in comparison with the Miyun observations in 2007, which was with an old version of model and a different anthropogenic emission inventory over China. Figure 3b displays the scatter plot of simulated vs. observed monthly-mean sulfate wet deposition fluxes from January 2009 to December 2010 at 5 EANET sites in China (Fig. 3c). The model reproduces the annual-mean sulfate wet deposition fluxes with a high correlation of 0.83 and small negative bias of −9 %. Seasonally, the model tends to overestimate sulfate wet deposition fluxes in the winter (bias = 30 %; $R$ = 0.63), but underestimate them in other seasons ($R$ = 0.8 ∼ 0.88, biases = −10 % ∼ −19 %). In summary, through comparison of the model results with satellite-derived AOD, surface sulfate observations at a rural site, and sulfate wet deposition fluxes for 5 sites in China, we conclude that the model has some capability to reproduce the spatial and temporal distributions of sulfate over China with a small to moderate bias.

## 3 Efficiency of $SO_2$ emission control strategies

### 3.1 Simulation scenarios

In this study, one standard simulation using the 2010 MEIC inventory of Chinese emissions and four sensitivity simulations with different $SO_2$ emission reduction scenarios (S1–S4) are conducted, which are described in Table 1. The standard simulation is carried out for the period from January 2009 to December 2010, with the first year for spin up and the next year for analysis. $SO_2$ emissions from China in 2010 are 28.4 Tg in the standard simulation. All the emission reduction scenarios have an 8 % (2.3 Tg)





ACPD
15, 4083–4115, 2015



reduction in national total $SO_2$ emissions below their 2010 level, following the goal of the 12th FYP, but they differ in the spatial distributions of those reductions. In the S1 scenario, the 8 % emission reduction is implemented uniformly over the whole country; in the S2, S3, and S4 scenario, the 2.3 Tg reduction of $SO_2$ emissions is implemented by decreasing regional emissions from three sub-regions of China have the largest contributions to the national $SO_2$ emissions and highest sulfate concentrations (Zhang et al., 2012; Wang et al., 2013). The three regions are North China (NC, 33–42° N, 110–122° E, S2), South China (SC, 22–33° N, 110–122° E, S3) and Southwest China (SWC, 23–33° N, 102–110° E, S4) (Fig. 1). Since the baseline emissions from the three regions are different, the percentage of the emission reduction differs by region, being 21.3, 29.5 and 48.9 % of emissions from NC, SC and SWC, respectively. For the emission reduction scenarios, only a 3-month's initialization is conducted.

Following Lamsal et al. (2011) and Zhang et al. (2014), we define a relationship between the change of an impact metric ($X$) and the change of $SO_2$ emissions ($E$): $\frac{\Delta X}{X} = \beta \times \frac{\Delta E}{E}$, where $\Delta X$ is the change in the metric, the $X$ can be surface sulfate concentrations, population-weighted sulfate concentration, or sulfur outflow fluxes from China to Western Pacific, and $\frac{\Delta X}{X}$ is the relative change of the metric; $\Delta E$ is the change of $SO_2$ emissions; $\frac{\Delta E}{E}$ is the relative emission change, which is 0.08 for all the emission reduction scenarios on the national scale; $\beta$ is a unitless term describing the relative changes of the metrics of concern in response to a 1 % change in $SO_2$ emissions. We call $\beta$ the efficiency factor, and it is used to compare the sensitivity of each metric to $SO_2$ emission changes between different emission reduction scenarios. The larger $\beta$, the larger impact $SO_2$ emission changes will have on the related metrics. $\beta$ tends to be $\leq 1$ because the relative rate of change in sulfate will not exceed that of $SO_2$ emissions. Considering that the emission reduction is regional-specific in S2–S4 scenarios, a regional-specific efficiency factor $\beta_{r,A-B}$ is also defined: $\left(\frac{\Delta X}{X}\right)_B = \beta_{r,A-B} \times \left(\frac{\Delta E}{E}\right)_A$, where $A$ denotes the region where emissions are reduced, and $B$ denotes the region where the impact is evaluated. For example, $\beta_{r,NC-SC}$ means the sensitivity of sulfate concentrations over SC to $SO_2$ emission reductions over NC. Here the regional $\frac{\Delta E}{E}$ is





ACPD
15, 4083–4115, 2015



0.08 for all the regions in S1, 0.213 for NC in S2, 0.295 for SC in S3 and 0.489 for SWC in S4 scenario. Since the S1 scenario does not have a regional-specific reduction in emissions, the regional sensitivity factor is simply $\beta_{r,B}$. All the $\beta$ and $\beta_{r,A-B}$ are displayed in Fig. 4.

### 3.2 Response of surface sulfate concentrations

In the S1 scenario, a uniform 8 % of reduction in $SO_2$ emissions (totally 2.3 Tg) over China results in a 5.7 % decrease of the national mean surface sulfate concentration, and the corresponding efficiency factor $\beta$ is 0.71 for the national mean sulfate concentration (Fig. 4a). The reduction of regional-mean sulfate concentration ranges from 6.2 % in SC ($\beta_{r,SC}$ = 0.78) to 7.2 % in NC ($\beta_{r,NC}$ = 0.9). The regional efficiency factors of sulfate over NC, SC and SWC are all greater than the national one, indicating higher emission control efficiency for regions with higher emissions. Seasonally, sulfate concentration decrease is smaller in winter than summer at all three regions, indicating that $SO_2$ emission changes have larger influence on sulfate in summer.

In the S2 scenario, $SO_2$ emissions from NC are reduced by 21.3 %, equivalent to a reduction of 2.3 Tg or 8 % of the national total, while emissions from the rest of the country remain unchanged. Annually, the S2 scenario results in a 14.4, 4.9 and 3.0 % decrease of sulfate concentrations over NC, SC, and SWC, respectively. $\beta$ for national mean sulfate concentration is 0.76, larger than that in S1 (0.71). The regional sulfate efficiency factors ($\beta_r$) to $SO_2$ emission change over NC are: $\beta_{r,NC-NC}$ = 0.68, $\beta_{r,NC-SC}$ = 0.23, and $\beta_{r,NC-SWC}$ = 0.14 (Fig. 4b and c). The $\beta_{r,NC-NC}$ in the S2 scenario is smaller than $\beta_{r,NC}$ in S1, because the latter includes reduced transport of sulfate resulting from lower emissions outside NC. The fact that $\beta_{r,NC-SC}$ and $\beta_{r,NC-SWC}$ are both significantly larger than zero indicates the important impact of NC emissions on sulfate concentrations over other regions by way of inter-regional transport. A comparison between $\beta_{r,NC-SC}$ and $\beta_{r,NC-SWC}$ provides a clear indication that $SO_2$ emissions from NC has a larger influence on sulfate concentrations over SC than those over SWC ($\beta_{r,NC-SC} > \beta_{r,NC-SWC}$, Fig. 4c).





ACPD
15, 4083–4115, 2015



In the S3 scenario in which $SO_2$ emissions from SC are reduced by 2.3 Tg or 29.5 %, the efficiency factor of national mean sulfate concentration is 0.69, smaller than that of S1 and S2. There is a 14.8 % decrease of sulfate concentrations over SC and the $\beta_{r,SC-SC}$ is 0.50, which compared with $\beta_{r,NC-NC}$ of 0.68 in S2 indicates that sulfate over SC is relatively less sensitive to within-region $SO_2$ emission change than that over NC. The regional efficiency factor of sulfate over NC to changing SC emissions ($\beta_{r,SC-NC}$) is 0.14 for the annual mean, lower than $\beta_{r,NC-SC}$ of 0.23 derived from S2. Seasonally, $SO_2$ emissions from SC have a larger influence on sulfate over NC in summer ($\beta_{r,SC-NC}$ = 0.16) than winter ($\beta_{r,SC-NC}$ = 0.11), because of different prevailing wind directions in the two seasons. Sulfate concentrations over SWC are less influenced by changing $SO_2$ emissions from SC, with a $\beta_{r,SC-SWC}$ of only 0.05.

The S4 scenario has the least effect on national mean sulfate concentration ($\beta$ = 0.68), despite of a 48.9 % reduction of $SO_2$ emissions from SWC. Sulfate concentrations over SWC have a relatively small efficiency factor to within-region $SO_2$ emission changes with the $\beta_{r,SWC-SWC}$ of 0.50. $\beta_{r,SWC-NC}$ and $\beta_{r,SWC-SC}$ are both less than 0.05, indicating the limited impact of $SO_2$ emissions on other regions due to the terrain of Sichuan Basin.

To summarize the above analysis of the four emission scenarios, we find that among the three regions selected, sulfate over NC is most sensitive to within-region emission changes ($\beta_{r,NC-NC}$ = 0.68, $\beta_{r,SC-SC}$ = 0.5, $\beta_{r,SWC-SWC}$ = 0.50), and $SO_2$ emission reductions over NC also have the largest influence on adjacent regions with $\beta_{r,NC-SC}$ and $\beta_{r,NC-SWC}$ the largest among the regional efficiency factors of inter-regional transport. As a result, the national-mean $\beta$ is highest in the S2 scenario (0.76), followed by S1 (0.71). This indicates that a nationwide uniform reduction of $SO_2$ emissions may not be the most effective way to reduce sulfate concentrations, and $SO_2$ emission reduction over NC should receive higher priority in the national policies.





ACPD
15, 4083–4115, 2015



### 3.3 Response of population-weighted sulfate concentration

Compared with the area-mean sulfate concentration, the population-weighted sulfate concentration (PWC) is a better metric to reflect the public exposure to atmospheric sulfate aerosols because it considers the spatial heterogeneity of population distribution. The PWC is calculated for each province by two steps: first multiplying the surface sulfate concentration by the population data (Stedman et al., 2002) over China estimated by SEDAC (SocioEconomic Data and Applications Center, http://sedac.ciesin.columbia.edu/data/collection/gpw-v3) for the year 2010, then summing up the values of all grid cells and dividing the sum by the total population to get the PWC. The original population data from the SEDAC database is at the resolution of about 5 km × 5 km ((1/24)° × (1/24)°). We regridded them to the resolution of 0.5° × 0.667° to match up with that of the sulfate concentrations from the model.

The annual mean sulfate concentrations and PWC are displayed in Fig. 5 by province. Higher sulfate concentrations and PWCs occur over the east and southwest part of China, in accordance with the spatial distribution of anthropogenic $SO_2$ emissions (cf. Fig. 1). The annual mean sulfate concentration is highest over SWC (9.9 $\mu g\,m^{-3}$), followed by NC (9.7 $\mu g\,m^{-3}$) and SC (8.1 $\mu g\,m^{-3}$). The highest PWC occurs in Chongqing and Sichuan province in SWC and the Hubei province in SC. The annual mean PWC over NC, SC and SWC is 11.2, 9.8 and 12.7 $\mu g\,m^{-3}$, respectively. The correlation between sulfate concentration and population density is stronger over SC and SWC than that over NC. As a result, SWC and SC exert higher weightings in the PWC metric than in the concentration metric.

The effects of the four emission scenarios on PWC in China are summarized in Table 2. The S3 scenario shows the largest decrease of PWC, with an 8.3 % reduction in mean PWC of the three regions mean and 7.8 % for the whole country. The S2 scenario has the second-largest impact, with the corresponding change of 7.6 and 7.5 % respectively. The efficiency factor of the national mean PWC is highest in S3 (0.98) and lowest in S1 (0.81). This regional difference indicates that $SO_2$ emission





ACPD
15, 4083–4115, 2015



reductions in SC (i.e., S3) is the most effective way to reduce human exposure to ambient sulfate aerosols, while the national-mean scenario (S1) is the least effective.

### 3.4 Response of sulfur outflow to the Pacific

We calculate the sulfur flux to Western Pacific in each scenario in winter and spring seasons, when the export of pollutants from China is most significant. The sulfur flux is defined for the tropospheric plane at 123° E extending from 22 to 42° N and includes both $SO_2$ and sulfate. Figure 6a displays the seasonal fluxes of each scenario. The standard simulation gives a flux of 490 kt S month$^{-1}$ in winter and 450 kt S month$^{-1}$ in spring. Compared with the standard simulation, the S1 scenario shows a 5.4 % decrease of sulfur flux in winter and 5.3 % in spring, with the mean value of $\beta$ being 0.67 for average fluxes of the two seasons. The S2 scenario shows the largest sulfur flux decrease of 7.2 % in winter and 8.0 % in spring and mean $\beta$ of 0.95, indicating that $SO_2$ emission control over NC has the strongest effects on reducing sulfur fluxes to the Western Pacific. The S3 and S4 scenarios have a much smaller impact compared to S1 and S2, and the S3 scenario results in the least response ($\beta$ = 0.50). This can be explained by the contribution of each region to the transport fluxes, which will be discussed in Sect. 4.2.

In summary, the comparison between the different spatial-realizations of the same amount of $SO_2$ emission reduction for China reveals different impacts not only by region but also by the impact metrics of choice. Reducing $SO_2$ emissions over NC results in the highest efficiency in reducing surface sulfate concentration in China as a whole with an efficiency factor of 0.76 as well as in reducing transport of sulfur to Western Pacific with the mean $\beta$ of 0.95. On the other hand, the sensitivity of population-weighted sulfate concentration is highest in the S3 scenario ($\beta$ = 0.98), so $SO_2$ emission control in SC is most effective to reduce human exposure to sulfate aerosols over China.





ACPD
15, 4083–4115, 2015



## 4 Regional differences in sulfur chemistry and transport

To better understand mechanistically the regional differences in the efficiency factors presented in Sect. 3, we investigate in this section the regional differences in the conversion of $SO_2$ to sulfate and inter-regional transport of the major sulfur compounds ($SO_2$ and sulfate) on the basis of GEOS-Chem model outputs. Sensitivity tests of our findings to meteorology and $SO_2$ emissions are also presented.

### 4.1 $SO_2$ conversion to sulfate

We have presented in Sect. 3.2 that the sensitivity of sulfate concentrations to local $SO_2$ emission changes differs from region to region, and the regional efficiency factor of $SO_2$ emission control is larger in NC ($\beta_{r,\,NC-NC}$) than other regions (i.e., $\beta_{r,\,SC-SC}$ and $\beta_{r,\,SWC-SWC}$). Here we attribute this difference to regional characteristics of sulfate chemistry using the GEOS-Chem model. As described in Sect. 2.1, in the model $SO_2$ is oxidized by OH to form sulfate in the gas phase, or by $H_2O_2$ and $O_3$ in the aqueous phase. The two pathways are the main source of atmospheric sulfate. The direct oxidation of $SO_2$ by $O_2$ catalyzed by transition metals (Alexander et al., 2009) and the heterogeneous reaction of $SO_2$ on pre-existing aerosols (Wang et al., 2014) are not included in current simulation. Globally aqueous phase oxidation plays a larger role than gas phase oxidation in sulfate formation (Unger et al., 2006), while their relative contributions vary regionally and seasonally. In the standard simulation, aqueous phase oxidation of $SO_2$ contributes 45, 64 and 73 % to sulfate over NC, SC and SWC, respectively. $H_2O_2$ oxidation makes up more than 90 % of aqueous phase oxidation for all the three regions. Barth and Church (1999) reported a more than 80 % contribution of aqueous phase oxidation to sulfate over Southeast China. Increasing emissions of $NO_x$ and hydrocarbons from China since the 1990s are expected to increase the relative importance of gas phase oxidation for sulfate (Berglen et al., 2004; Unger et al., 2006), which explains the lower fraction of aqueous oxidation in our study.





ACPD
15, 4083–4115, 2015



Table 3 presents the relative changes of $SO_2$ emissions, $SO_2$ oxidation rate (gas and aqueous phase and total of them), and sulfate concentrations in the regional-specific scenarios (S2–S4) compared with the standard simulation. Reducing $SO_2$ emissions has different influences on gas and aqueous oxidation. Over all three regions, the relative decrease of gas phase oxidation is greater than that of aqueous oxidation, so the region with higher contribution from gas phase oxidation will show a larger sensitivity of sulfate to $SO_2$ emissions reduction; in our study, NC is the region with the largest fraction of gas phase oxidation. Adopting the relationship between the impact metric and $SO_2$ emission changes defined in Sect. 3, we derive the regional sensitivity of $SO_2$ oxidation to be 0.76 for NC (S2), larger than that of 0.67 for SC (S3) and 0.64 for SWC (S4), explaining the larger response of sulfate over NC to within-region $SO_2$ emissions than the other two regions.

Roelofs et al. (1998) and Berglen et al. (2004) compared the simulated sulfate concentrations from a model simulation using prescribed concentrations of oxidants with those using coupled oxidants. They showed that over regions with high $SO_2$ emissions, simulated sulfate concentration with fixed oxidants are higher than that from the simulation using coupled oxidants. They also found that in the run with prescribed oxidants, $H_2O_2$ oxidation became more important, while gas phase OH oxidation was little affected. Their results indicate that regions with high $SO_2$ emissions (like China) are oxidation limited, especially for the aqueous phase $H_2O_2$ oxidation pathway. Under the oxidation limited conditions, the oxidation rate of $SO_2$ is less sensitive to $SO_2$ emission changes, so changing $SO_2$ emissions will have a larger influence on gas phase oxidation than aqueous phase oxidation. Proportion of gas phase oxidation in NC (55 %) is much larger than that in SC (36 %) and SWC (27 %), so $SO_2$ oxidation rates in NC is more sensitive to $SO_2$ emission changes than SC and SWC.

### 4.2 Sulfur transport

The decrease of sulfate concentrations for each region is less than that attributed to within-region $SO_2$ oxidation and the difference is due to the transport of sulfur between





ACPD
15, 4083–4115, 2015



regions. To further separate the impact of within-region vs. inter-regional transport on sulfate concentrations by region, we conducted additional model experiments in which $SO_2$ emissions from NC, SC and SWC are zeroed off separately. The difference of sulfate concentrations between the standard simulation and each of the zeroing-off model experiments represents the contribution of $SO_2$ emissions from the corresponding region with zero emissions. The resulting decomposition of monthly mean sulfate concentrations by source regions of $SO_2$ is displayed in Fig. 7 for NC, SC, and SWC separately.

For the annual average, within-region $SO_2$ emissions contribute 68 % of sulfate concentrations over NC (Fig. 7a), followed by 15 % from SC emissions. Seasonally, contributions from SC emissions range from 10 % during winter to 17 % during summer. $SO_2$ emissions from SWC have a small influence (4 %) on sulfate over NC, and the remaining 13 % of sulfate over NC is from other sources. For SC (Fig. 7b), only 59 % of sulfate comes from $SO_2$ emitted within SC. NC is an important source region for sulfate over SC, contributing 23 % annually and ranging from 11 % in winter to 30 % in summer. Transport from SWC is very small of only 4 %. For SWC, within-region emissions provide 61 % of sulfate (Fig. 7c), while transport from NC and SC contributes 10 and 8 %, respectively, with the remaining 21 % from other sources. The overall contribution of the inter-regional transport between the three regions is 19, 27, and 18 % to sulfate over NC, SC, and SWC, respectively. Among all the inter-regional transport of sulfate examined here, $SO_2$ emissions from NC exert the largest impacts to sulfate concentrations in other regions, contributing 23 and 10 % to sulfate over SC and SWC, respectively. This explains why $\beta_{r,NC-SC}$ and $\beta_{r,NC-SWC}$ derived from the S2 scenario are larger than the regional sensitivity factors of inter-regional transport in other emission scenarios. As a result, for a given amount of $SO_2$ emission reduction in China, implementing it over NC is found most effective in getting the largest benefit of reducing surface sulfate concentrations over China as a whole.

We further quantify the contribution of each region to the transport fluxes of total sulfur ($SO_2$ + sulfate) to the Western Pacific for winter, spring and the mean of the two





ACPD
15, 4083–4115, 2015



seasons (Fig. 6b). NC is the largest contributor and contributes ~ 40 % of total fluxes for each season. This explains the largest sensitivity factor of the export fluxes to NC emissions in the S2 scenario ($\beta = 0.95$). The contribution from SWC is the second largest, being 17 % in spring and 24.1 % in winter and a mean of 20.7 % for the two seasons. Most of the export fluxes from SWC are found above the boundary layer and as such they have a small effect on surface sulfate concentrations over NC or SC. SC contributes the least (20 %) to the export fluxes among the three regions, resulting in the smallest sensitivity factor of sulfur export flux to the Western Pacific ($\beta = 0.50$) in S3 scenario.

### 4.3 Robustness test

The chemistry of $SO_2$ conversion to sulfate and the transport of sulfur compounds are dependent on both meteorology and emissions. We used a single year's meteorology and emissions (2010) to derive the efficiency factors. To assess the uncertainty of our analysis to the choice of meteorology and the magnitude of emission reductions, sensitivity tests were carried out by changing the year of meteorology to 2009 and by doubling the amount of $SO_2$ emissions reductions. The national mean sensitivity factor of surface sulfate concentration, population-weighted sulfate concentration and eastward transport fluxes are calculated and compared with that from the S1–S4 emission reduction scenarios.

First, to examine the sensitivity of the model results to the meteorological fields, we conducted a series of one year test simulations with the 2009 meteorology. In the tests, we use the same emissions as in the standard simulation and the S1–S4 scenarios. With the 2009 meteorology, the national mean sulfate concentration and eastward transport fluxes are also most sensitive to $SO_2$ emission reduction from NC (Fig. 4a, green short line). The discrepancy in the value of $\beta$ between simulation with 2009 and 2010 meteorology is within 5 %. The efficiency factors for national mean sulfate concentration and sulfur flux are 0.78 and 0.94, respectively, compared with the 0.76 and 0.95 from the 2010 meteorology. $SO_2$ emission reduction in SC is most effective in re-





ACPD
15, 4083–4115, 2015



ducing people's exposure to sulfate aerosols with national mean $\beta$ of 0.94 with 2009 meteorology, and it is 0.98 from 2010 meteorology.

Second, the magnitude of $SO_2$ emissions reduction is doubled in each of the S1–S4 scenarios to check the sensitivity of model results to emissions. These tests are run for one year and with the 2010 meteorology. The efficiency factor for national mean sulfate concentration, PWC and sulfur transport fluxes to the Western Pacific from this test are displayed in Fig. 4a with yellow short line. When $SO_2$ emission reduction is doubled, the national mean sulfate concentration and export sulfur fluxes are also most sensitive to $SO_2$ emission reduction from NC, and $\beta$ for national mean PWC is largest when $SO_2$ emission reduced from SC. However, there is a relatively significant decrease in the value of $\beta$, especially for national mean sulfate concentration and PWC (more than 20 %). This indicates that $SO_2$ oxidation rate becomes less sensitive when $SO_2$ emission reduction is greater.

In summary, we find $SO_2$ emissions reduction has a larger influence on gas phase oxidation than aqueous phase oxidation. Because sulfate in NC has the largest relative contribution from gas phase oxidation, NC shows the largest sensitivity to within-region $SO_2$ emission changes. Besides, inter-regional transport contributes 18 ∼ 27 % of sulfate over the three regions. $SO_2$ emissions from NC contribute 23 and 10 % to sulfate over SC and SWC, respectively, which are the largest among all the inter-regional transport of sulfate. This explains why $\beta_{r,\,NC-SC}$ and $\beta_{r,\,NC-SWC}$ are the largest among all the efficiency factors to external emission changes (Sect. 3.2 and Fig. 4c). $SO_2$ emissions from NC contributes the most (∼ 40 %) to the sulfur transport fluxes from China to the Western Pacific, resulting in the largest sensitivity factor (0.95) of the transport flux in S2 scenario. Contribution from SC is the least (20 %), so $SO_2$ emission reduction from SC has least influence on the transport flux. The robustness tests demonstrate that our results are robust with different meteorology year and different magnitude of $SO_2$ emission reduction.





ACPD
15, 4083–4115, 2015



## 5 Conclusion and discussion

The same amount of $SO_2$ emission reduction (2.3 Tg, 8 % of total $SO_2$ emission from China in 2010, following the 12th FYP) has been implemented on the whole China and three sub-regions of China (NC, SC and SWC) to investigate the emission control efficiencies in different regions. The GEOS-Chem chemical transport model is used in this study to quantify response of sulfate to $SO_2$ emission changes.

National mean and inter-regional efficiency factors ($\beta$ and $\beta_r$) are defined as the percentage change of the concerned metrics caused by 1 % decrease of $SO_2$ emission changes. The metrics include surface sulfate concentration, the population-weighted sulfate concentration and sulfur transport from China to the Western Pacific. We find that $SO_2$ emission reduction over NC (S2 scenario) is most effective in reducing mean sulfate concentration over China as a whole with the highest national-mean $\beta$ of 0.76, which can be explained in two aspects. On one hand, $SO_2$ oxidation in gas phase is found to be more sensitive to changes of $SO_2$ emission than that in aqueous phase, and NC is the region with the largest fraction of gas phase $SO_2$ oxidation. This makes sulfate over NC most sensitive to within-region emission changes with the largest efficiency factor ($\beta_{r,\,NC-NC} = 0.68$, $\beta_{r,\,SC-SC} = 0.5$, $\beta_{r,\,SWC-SWC} = 0.50$). On the other hand, comparison of inter-regional sulfate transport reveals that $SO_2$ emissions from NC exert the largest impacts to sulfate concentrations in other regions (23 % for SC and 10 % for SWC). This leads to $\beta_{r,\,NC-SC}$ and $\beta_{r,\,NC-SWC}$ as the largest among the regional efficiency factors of inter-regional transport.

Among the three regions, NC contributes most ($\sim$ 40 %) to the transport fluxes of sulfur from China to the Western Pacific, so the Western Pacific region benefits most from $SO_2$ reduction in NC with the mean $\beta$ of 0.95. Contribution from SC is least among the three regions, resulting in the smallest efficiency factor of sulfur export flux to the Western Pacific ($\beta = 0.50$) in S3 scenario. We also find that $SO_2$ emission control in SC is most effective to reduce human exposure to sulfate aerosols over China for the sensitivity of population-weighted sulfate concentration is highest in the S3 scenario





ACPD
15, 4083–4115, 2015



($\beta$ = 0.98). The efficiency factors and their spatial differences are found to be robust and not dependent on the year of meteorology or the magnitude of $SO_2$ emissions change.

We recommend that a nationwide uniform reduction of $SO_2$ emissions may not result in the greatest emission control efficiency. $SO_2$ emission reduction over NC should receive higher priority in the national policies to reduce surface sulfate concentration and sulfur transport fluxes to the Western Pacific, while $SO_2$ emission reduction over SC is most favorable to reduce people's exposure to sulfate aerosols.

*Acknowledgements.* This research was supported by the National Key Basic Research Program of China (2014CB441302), the CAS Strategic Priority Research Program (Grant No. XDA05100403), and the Beijing Nova Program (Z121109002512052). We thank the free use of surface measurements from EANET and AOD data from MODIS.

## References

Alexander, B., Park, R. J., Jacob, D. J., and Gong, S.: Transition metal-catalyzed oxidation of atmospheric sulfur: global implications for the sulfur budget, J. Geophys. Res., 114, D02309, doi:10.1029/2008JD010486, 2009.

Barth, M. C. and Church, A. T.: Regional and global distributions and lifetimes of sulfate aerosols from Mexico City and southeast China, J. Geophys. Res., 104, 30231–30239, 1999.

Benkovitz, C. M., Scholtz, M. T., Pacyna, J., Tarrasón, L., Dignon, J., Voldner, E. C., Spiro, P. A., Logan, J. A., and Graedel, T. E.: Global gridded inventories of anthropogenic emissions of sulfur and nitrogen, J. Geophys. Res., 101, 29239–29253, doi:10.1029/96JD00126, 1996.

Berglen, T. F., Berntsen, T. K., Isaksen, I. S. A., and Sundet, J. K.: A global model of the coupled sulfur/oxidant chemistry in the troposphere: the sulfur cycle, J. Geophys. Res., 109, D19310, doi:10.1029/2003JD003948, 2004.

Chen, D., Wang, Y., McElroy, M. B., He, K., Yantosca, R. M., and Le Sager, P.: Regional CO pollution and export in China simulated by the high-resolution nested-grid GEOS-Chem model, Atmos. Chem. Phys., 9, 3825–3839, doi:10.5194/acp-9-3825-2009, 2009.





ACPD
15, 4083–4115, 2015



Fairlie, T. D., Jacob, D. J., Dibb, J. E., Alexander, B., Avery, M. A., van Donkelaar, A., and Zhang, L.: Impact of mineral dust on nitrate, sulfate, and ozone in transpacific Asian pollution plumes, Atmos. Chem. Phys., 10, 3999–4012, doi:10.5194/acp-10-3999-2010, 2010.

Fountoukis, C. and Nenes, A.: ISORROPIA II: a computationally efficient thermodynamic equilibrium model for $K^+$–$Ca^{2+}$–$Mg^{2+}$–$NH_4^+$–$Na^+$–$SO_4^{2-}$–$NO_3^-$–$Cl^-$–$H_2O$ aerosols, Atmos. Chem. Phys., 7, 4639–4659, doi:10.5194/acp-7-4639-2007, 2007.

Heald., C. L., Jacob, D. J., Park, R. J., Alexander, B., Fairlie, T. D., Yantosca, R. M., and Chu, D. A.: Transpacific transport of Asian anthropogenic aerosols and its impact on surface air quality in the United Stades, J. Geophys. Res., 111, D14310, doi:10.1029/2005JD006847, 2006.

He, H., Li, C., Loughner, C. P., Li, Z., Krotkov, N. A., Yang, K., Wang, L., Zheng, Y., Bao, X., Zhao, G., and Dickerson, R. R.: $SO_2$ over central China: measurements, numerical simulations and the tropospheric sulfur budget, J. Geophys. Res., 117, D00K37, doi:10.1029/2011JD016473, 2012.

He, K. B.: Multi-resolution Emission Inventory for China (MEIC): model framework and 1990–2010 anthropogenic emissions, International Global Atmospheric Chemistry Conference, 17–21, September, Beijing, China, 2012.

Itahashi, S., Uno, I., Yumimoto, K., Irie, H., Osada, K., Ogata, K., Fukushima, H., Wang, Z., and Ohara, T.: Interannual variation in the fine-mode MODIS aerosol optical depth and its relationship to the changes in sulfur dioxide emissions in China between 2000 and 2010, Atmos. Chem. Phys., 12, 2631–2640, doi:10.5194/acp-12-2631-2012, 2012a.

Itahashi, S., Uno, I., and Kim, S.: Source contributions of sulfate aerosols over East Asia estimated by CMAQ-DDM, Environ. Sci. Technol., 46, 6733–6741, 2012b.

Lamsal, L. N., Martin, R. V., Padmanabhan, A., van Donkelaar, A., Zhang, Q., Sioris, C. E., Chance, K., Kurosu, T. P., and Newchurch, M. J.: Application of satellite observations for timely updates to global anthropogenic $NO_X$ emission inventories, Geophys. Res. Lett., 38, L05810, doi:10.1029/2010GL046476, 2011.

Li, C., Krotkov, N. A., Dickerson, R. R., Li, Z, Yang, K., and Chin, M.: Transport and evolution of a pollution plume from northern China: a satellite-based case study, J. Geophys. Res., 115, D00K03, doi:10.1029/2009JD012245, 2010.

Lou, S., Liao, H., and Zhu, B.: Impacts of aerosols on surface-layer ozone concentrations in China through heterogeneous reactions and changes in photolysis rates, Atmos. Environ., 85, 123–138, 2014.





ACPD
15, 4083–4115, 2015



Lu, Z., Zhang, Q., and Streets, D. G.: Sulfur dioxide and primary carbonaceous aerosol emissions in China and India, 1996–2010, Atmos. Chem. Phys., 11, 9839–9864, doi:10.5194/acp-11-9839-2011, 2011.

Manktelow, P. T., Mann, G. W., Carslaw, K. S., Spracklen, D. V., and Chipperfield, M. P.: Regional and global trends in sulfate aerosol since the 1980s, Geophys. Res. Lett., 34, L14803, doi:10.1029/2006GL028668, 2007.

Park, R. J., Jacob, D. J., Field, B. D., Yantosca, R. M., and Chin, M.: Natural transboundary pollution influences on sulfate-nitrate-ammonium aerosols in the United States: implications for policy, J. Geophys. Res., 109, D15204, doi:10.1029/2003JD004473, 2004.

Roelofs, G.-J., Lelieveld, J., and Ganzeveld, L.: Simulation of global sulfate distribution and the influence on effective cloud drop radii with a coupled photochemistry-sulfur cycle model, Tellus B, 50, 224–242, 1998.

Schreifels, J. J., Fu, Y., and Wilson, J. E.: Sulfur dioxide control in China: policy evolution during the 10th and 11th Five-Year Plans and lessons for the future, Energ. Policy, 48, 779–789, 2012.

Stedman, J. R., Grice, S., Kent, A., and Cooke, S.: GIS-based models for ambient PM exposure and health impact assessment for the UK, J. Phys. Conf. Ser., 151, 012002, doi:10.1088/1742-6596/151/1/012002, 2002.

Unger, N., Shindell, D. T., Koch, D. M., and Streets, D. G.: Cross influences of ozone and sulfate precursor emissions changes on air quality and climate, P. Natl. Acad. Sci. USA, 103, 4377–4380, 2006.

Wang, J., Xu, X., Henze, D. K., Zeng, J., Ji, Q., Tsay, S.-C., and Huang, J.: Top-down estimate of dust emissions through integration of MODIS and MISR aerosol retrievals with the GEOS-Chem adjoint model, Geophys. Res. Lett., 39, L08802, doi:10.1029/2012GL051136, 2012.

Wang, L. T., Wei, Z., Yang, J., Zhang, Y., Zhang, F. F., Su, J., Meng, C. C., and Zhang, Q.: The 2013 severe haze over southern Hebei, China: model evaluation, source apportionment, and policy implications, Atmos. Chem. Phys., 14, 3151–3173, doi:10.5194/acp-14-3151-2014, 2014.

Wang, Y., McElroy, M. B., Jacob, D. J., and Yantosca, R. M.: A nested grid formulation for chemical transport over Asia: applications to CO, J. Geophys. Res., 109, D22307, doi:10.1029/2004JD005237, 2004.





ACPD
15, 4083–4115, 2015



Wang, Y., Zhang, Q. Q., He, K., Zhang, Q., and Chai, L.: Sulfate-nitrate-ammonium aerosols over China: response to 2000–2015 emission changes of sulfur dioxide, nitrogen oxides, and ammonia, Atmos. Chem. Phys., 13, 2635–2652, doi:10.5194/acp-13-2635-2013, 2013.

Wang, Y., Zhang, Q. Q., Jiang, J., Zhou, W., Wang, B., He, K., Duan, F., Zhang, Q., Philip, S., and Xie, Y.: Enhanced sulfate formation during China's severe winter haze episode in January 2013 missing from current models, J. Geophys. Res., 119, 10425–10440, doi:10.1002/2013JD021426, 2014.

Zhang, H., Wu, S., Huang, Y., and Wang, Y.: Effects of stratospheric ozone recovery on photochemistry and ozone air quality in the troposphere, Atmos. Chem. Phys, 14, 4079–4086, doi:10.5194/acp-14-4079-2014, 2014.

Zhang, Q., Streets, D. G., Carmichael, G. R., He, K. B., Huo, H., Kannari, A., Klimont, Z., Park, I. S., Reddy, S., Fu, J. S., Chen, D., Duan, L., Lei, Y., Wang, L. T., and Yao, Z. L.: Asian emissions in 2006 for the NASA INTEX-B mission, Atmos. Chem. Phys., 9, 5131–5153, doi:10.5194/acp-9-5131-2009, 2009.

Zhang, X. Y., Wang, Y. Q., Niu, T., Zhang, X. C., Gong, S. L., Zhang, Y. M., and Sun, J. Y.: Atmospheric aerosol compositions in China: spatial/temporal variability, chemical signature, regional haze distribution and comparisons with global aerosols, Atmos. Chem. Phys., 12, 779–799, doi:10.5194/acp-12-779-2012, 2012.





ACPD
15, 4083–4115, 2015



**Table 1.** Simulation scenarios and $SO_2$ emission in each study.

| Simulation scenario | description | $SO_2$ emission (Tg) | | | |
|---|---|---|---|---|---|
| | | China | NC | SC | SWC |
| standard | Standard, 2010 inventory | 28.4 | 10.8 | 7.8 | 4.7 |
| S1 | $SO_2$ emission is reduced uniformly across China by 8 % (2.3 Tg) | 26.1 | 9.9 | 7.2 | 4.3 |
| S2 | Implement 2.3 Tg $SO_2$ reduction on NC, emission from other regions unchanged | 26.1 | 8.5 | 7.8 | 4.7 |
| S3 | Implement 2.3 Tg $SO_2$ reduction on SC, emission from other regions unchanged | 26.1 | 10.8 | 5.5 | 4.7 |
| S4 | Implement 2.3 Tg $SO_2$ reduction on SWC, emission from other regions unchanged | 26.1 | 10.8 | 7.8 | 2.4 |





ACPD
15, 4083–4115, 2015



**Table 2.** Change in population-weighted sulfate concentrations, $\mu g\,m^{-3}$.

| | standard simulation | Difference with the standard simulation S1 | S2 | S3 | S4 |
|---|---|---|---|---|---|
| NC + SC + SWC | 10.9 | −6.7 % | −7.6 % | −8.3 % | −7.1 % |
| China | 9.7 | −6.6 % | −7.5 % | −7.8 % | −6.9 % |





ACPD
15, 4083–4115, 2015



**Table 3.** Percentage changes of $SO_2$ conversion to sulfate and sulfate concentration over NC, SC and SWC in response to within-region $SO_2$ emission changes.

| | $SO_2$ | $SO_2$ conversion | | | Sulfate |
|---|---|---|---|---|---|
| | emission | Gas phase | Aqueous phase | total | concentration |
| NC (S2) | −21.3 % | −20.6 % | −10.4 % | −16.1 % | −14.4 % |
| SC (S3) | −29.5 % | −22.6 % | −17.1 % | −19.9 % | −14.8 % |
| SWC (S4) | −48.9 % | −41.8 % | −30.1 % | −31.4 % | −24.5 % |





ACPD
15, 4083–4115, 2015



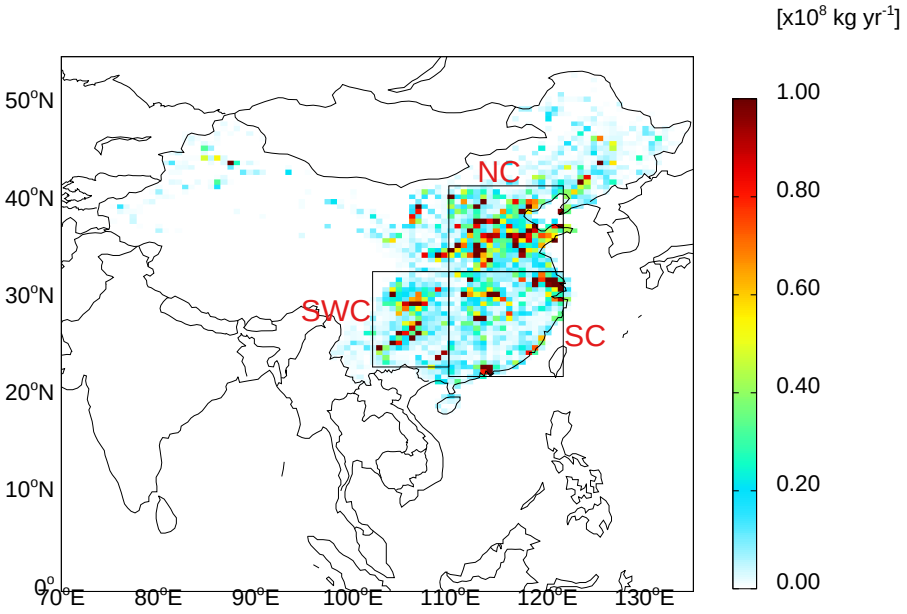


**Figure 1.** $SO_2$ emissions from China in the year of 2010.





ACPD
15, 4083–4115, 2015

Regional differences in Chinese $SO_2$ emission control efficiency

Q. Q. Zhang et al.



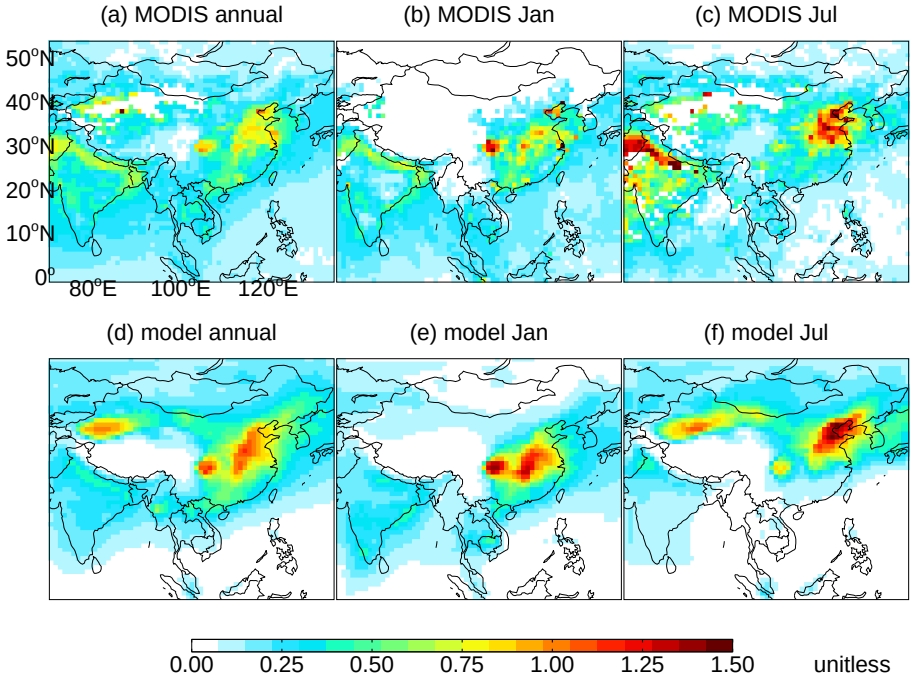


**Figure 2.** Aerosol optical depth (AOD) over East Asia from MODIS for **(a)** 2010 annual mean, **(b)** January, and **(c)** July, and from the GEOS-Chem model: **(d)** annual mean, **(e)** January, and **(f)** July.





ACPD
15, 4083–4115, 2015



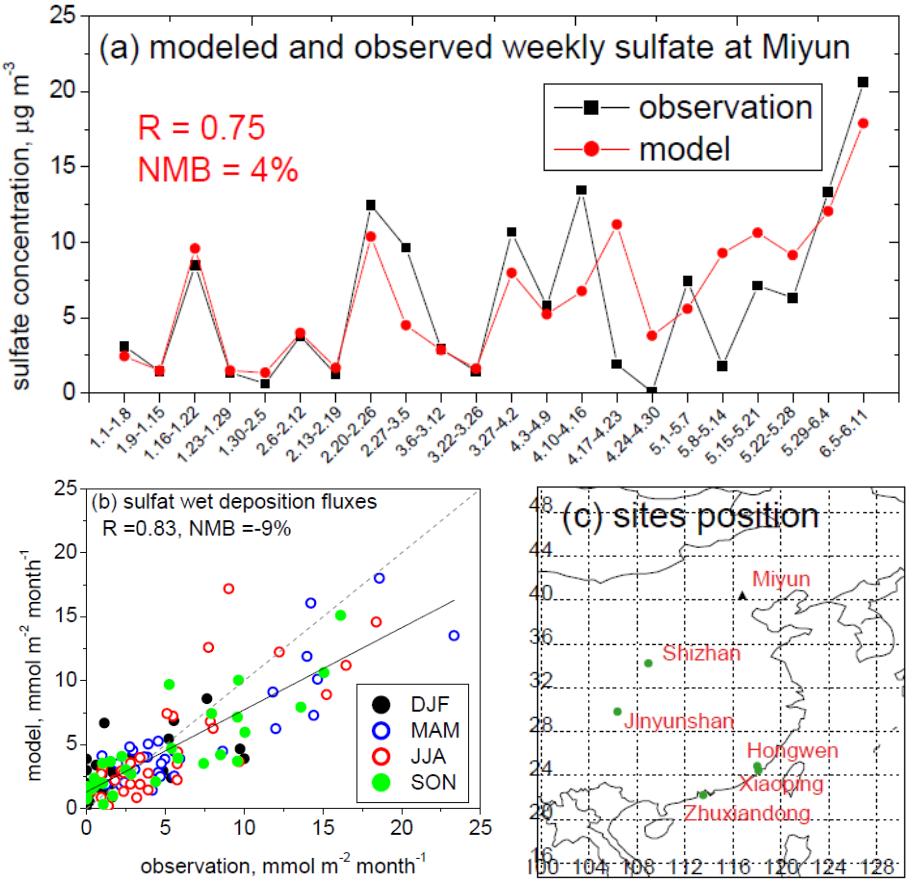


**Figure 3. (a)** Simulated and observed weekly sulfate concentration at the Miyun site from January to June 2010; **(b)** scatter plot of simulated vs. observed sulfate wet deposition fluxes in 5 sites over China, from January 2009 to December 2010; **(c)** the locations of the observing sites.





ACPD
15, 4083–4115, 2015



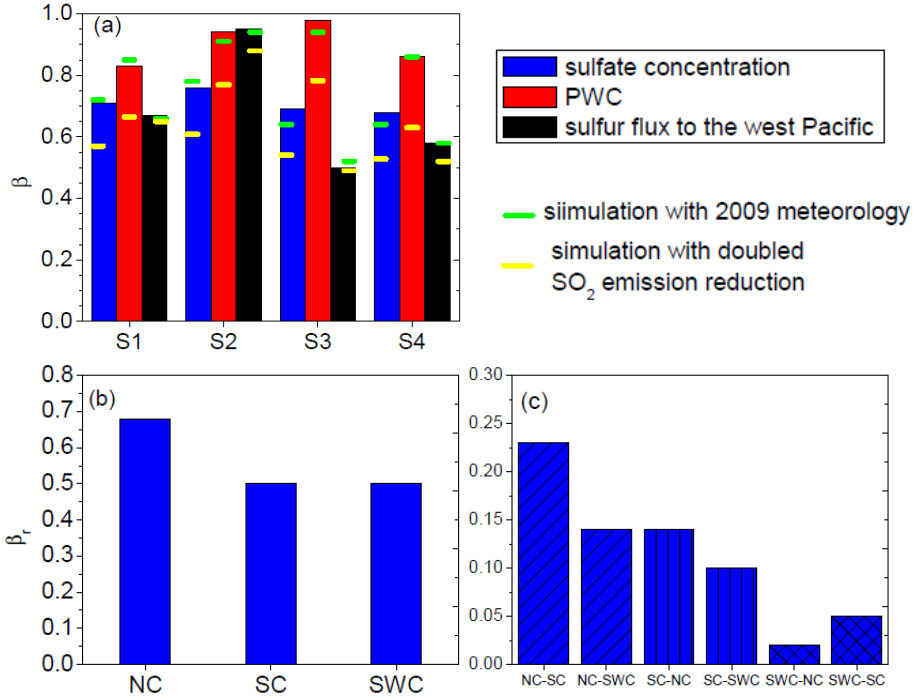


**Figure 4.** Emission control efficiency factors ($\beta$) of national mean sulfate concentrations, population-weighted sulfate concentrations and sulfur fluxes from China to the west Pacific to 8 % $SO_2$ emission reductions in S1–S4 simulation scenarios **(a)**, and regional sensitivity factors ($\beta_r$) of sulfate concentrations over NC, SC and SWC to **(b)** within-region $SO_2$ emission changes and **(c)** external $SO_2$ emission changes. The efficiency factor of national mean sulfate concentrations, population-weighted sulfate concentrations and eastward sulfur transport fluxes in the robustness tests are presented in **(a)**, and the green short line represents results from simulation with meteorology for 2009, the yellow short line represents results from doubled magnitude of $SO_2$ emission reduction simulation.





ACPD
15, 4083–4115, 2015



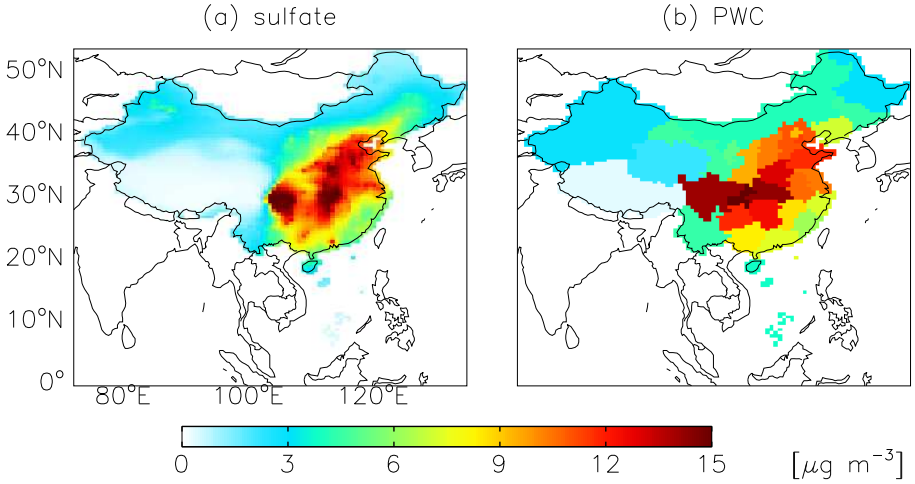


**Figure 5.** Annual mean sulfate concentration and population-weighted sulfate concentration over China (sulfate and population data of Taiwan Province is not available).





ACPD
15, 4083–4115, 2015



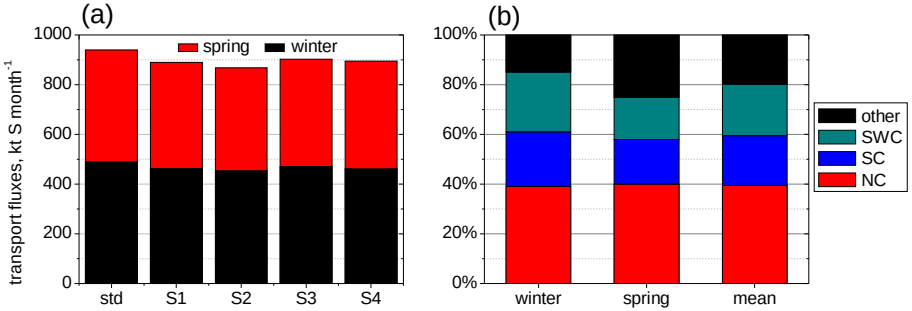


**Figure 6. (a)** Sulfur ($SO_2$ + sulfate) flux at 123° E, 22–42° N from China to the Western Pacific, and **(b)** percentage contribution of NC, SC and SWC to sulfur ($SO_2$ + sulfate) transport fluxes from China to the Western Pacific.





ACPD
15, 4083–4115, 2015



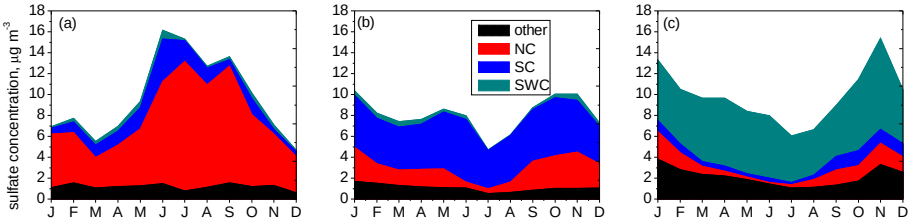


**Figure 7.** Monthly and regional mean sulfate concentrations over **(a)** NC, **(b)** SC and **(c)** SWC, with contributions from within-region and regional transport.





ACPD
15, 4083–4115, 2015